

LAMINAR COMBINED CONVECTION FROM A HORIZONTAL CYLINDER—PARALLEL AND CONTRA FLOW REGIMES

H. M. BADR

Mechanical Engineering Department, University of Petroleum & Minerals, Dhahran, Saudi Arabia

(Received 29 November 1982 and in final form 11 March 1983)

Abstract—The laminar combined convection heat transfer from an isothermal horizontal circular cylinder is studied for the two cases when the forced flow is directed either vertically upward (parallel flow) or vertically downward (contra flow). The investigation is based on the solution of the full vorticity transport equation together with the stream function and energy equations. The velocity and thermal boundary layers are developed in time until reaching steady conditions. The variations of vorticity and Nusselt number are obtained over all the cylinder surface including the zone beyond the separation point. The predicted values of the average Nusselt number are compared with the available experimental data and the agreement is satisfactory. The streamline and isotherm patterns are plotted for several cases to show some of the flow field characteristics.

NOMENCLATURE

a	cylinder radius
c	specific heat
f_n	functions defined in equation (8)
g	gravitational acceleration
g_n	functions defined in equation (8)
Gr	Grashof number, $g\beta(T_s - T_\infty)(2a)^3/\nu^2$
h, \bar{h}	local and average heat transfer coefficients
H_0, H_n	functions defined in equation (8)
k	thermal conductivity
Nu, \bar{Nu}	local and average Nusselt numbers
Pe	Péclet number, $Re Pr$
Pr	Prandtl number, $\mu c/k$
q	rate of heat transfer per unit area
r	dimensionless radial coordinate, r'/a
Re	Reynolds number, $2au_\infty/\nu$
t	dimensionless time
T	temperature
v_r, v_θ	radial and transverse components of velocity
u_∞	uniform stream velocity.
Greek symbols	
β	coefficient of volumetric thermal expansion
δ	constant defined following equation (11)
ξ	logarithmic radial coordinate, $\ln(r'/a)$
ρ	density
ν	kinematic viscosity
ϕ	dimensionless temperature, $(T - T_\infty)/(T_s - T_\infty)$
ψ	dimensionless stream function, ψ'/au_∞
θ	angular coordinate
ζ	dimensionless vorticity, $\zeta'a/au_\infty$.

INTRODUCTION

COMBINED forced and natural convection heat transfer from a circular cylinder continues to be one of the important problems due to its fundamental nature as

well as the many related engineering applications. In spite of the fact that a good number of experimental investigations were carried out in the past, it seems that most of the theoretical treatment of the problem is limited to cases in which the forced flow is directed vertically upward (parallel flow). Even though for this relatively simple case of parallel flow the solution of the problem, according to the literature, is incomplete since none of the previously presented theories succeeded to predict any information about the velocity and thermal fields beyond the point of separation. On the other hand, the solution of the problem when the forced flow is directed downward (contra flow) received, so far, very little success because the boundary-layer flow assumption may not be valid especially when buoyant forces are comparable to inertia forces.

The first theoretical study on combined convection from bodies in the existence of boundary-layer flows was carried out by Acrivos [1] who obtained the Nusselt number for the case of stagnation flow when Prandtl number $Pr \rightarrow 0$ or $Pr \rightarrow \infty$. Joshi and Sukhatme [2] introduced a method to study the problems of parallel and contra flows. The method is based on a series solution of the laminar boundary-layer equations. In their work the velocity distribution outside the boundary layer was assumed to be exactly the same as that of potential flow. Under the above assumptions their study was limited to the region from the forward stagnation point up to the point of separation only. Accordingly, the average Nusselt number over the cylinder surface could not be obtained. In Joshi and Sukhatme's work no study was carried out to investigate the accuracy and limitations of the boundary-layer simplifications as well as the assumptions of potential flow outside the boundary layer. Nakai and Okazaki [3] studied the problem of combined convection from a circular cylinder for the cases of parallel, cross and contra flows. Their analysis was limited to cases when Reynolds number, Re , and Grashof number, Gr , are very small and also when either forced convection or natural convection is

dominant. Their results were found to agree reasonably with experimental data for the case of parallel flow, however, a considerable difference was found in case of contra flow. Sparrow and Lee [4] considered the parallel flow regime and obtained a similarity solution based on using an approximate expression for the velocity variation outside the boundary layer. The local Nusselt number distribution was only obtained in the region upstream of the point of separation (from the forward stagnation point up to an angle of 70°). Merkin [5] studied the same problem by obtaining a numerical solution to the boundary-layer equations based on the assumption that $Re \gg 1$ and $Gr \gg 1$. The method was again restricted to the region preceding the point of separation since the boundary-layer equations are not valid beyond that point. Lately, Badr [6] presented a method to deal with the problem of cross combined convection from a circular cylinder. The method is based on the solution of the full Navier–Stokes and energy equations.

Numerous experimental investigations were carried out to study the effect of various parameters on the rate of heat transfer from a circular cylinder. The first comprehensive experimental work on this problem was carried out by Hatton *et al.* [7] who investigated combined convection from horizontal cylinders upto $Re = 45$ and Rayleigh number, $Ra = 10$. The effect of free stream direction on the heat transfer process was also investigated. A correlation based on vectorial summation of the forced and natural heat transfer effects was suggested. This correlation was found to fit the data reasonably well except when the flow direction approaches that of contra flow where the correlation fails to predict the Nusselt number. Gebhart and Pera [8] conducted experiments on the same problem, however, for very small Reynolds and Grashof numbers. A good survey of the work done on this problem prior to 1970 was found therein. Oosthuizen and Madan [9] considered the problem of parallel flow in the ranges of Reynolds number $10^2 < 3 \times 10^3$ and Grashof number $2.5 \times 10^4 < Gr < 3 \times 10^5$. Based on their experimental data a correlation for the average Nusselt number was obtained. An alternative correlation of the same data was obtained by Jackson and Yen [10] which was found to fit the data better especially at higher values of Gr/Re^2 . In another work by Oosthuizen and Madan [11] the effect of flow direction on the rate of heat transfer is investigated when the free stream makes an angle of $0^\circ, 90^\circ, 135^\circ$, and 180° with the direction of natural convection. No correlation was given in that work.

In the present work the problem of laminar combined convection from an isothermal horizontal circular cylinder is considered for the two cases of parallel and contra flows. The objective here is two-fold. First, to study the case of parallel flow in order to obtain the vorticity and local Nusselt number variation over all the cylinder surface. Second, to investigate the case of contra flow and show the details of the velocity and thermal boundary layers in addition to the effect of the different parameters on the streamline and isotherm patterns. Of special interest is to consider the cases in

which the effect of natural convection is of the same order of magnitude as that of forced convection.

PROBLEM STATEMENT

Consider the problem of a horizontal circular cylinder, of radius a , that has an isothermal surface, of temperature T_s , and is placed in a uniform free stream of temperature T_∞ and velocity u_∞ . The free stream is directed either vertically upward or vertically downward. The temperature difference $\Delta T (= T_s - T_\infty)$ is assumed to have a negligible effect on the fluid properties except for the buoyancy forces in the momentum equation. The cylinder is considered to be long enough so that the end effects can be neglected and accordingly the flow field can be assumed two-dimensional. Consider the line $\theta = 0$ to be the radius through the rearmost point on the cylinder surface viewed from the upstream direction (the free stream will always be in the direction $\theta = 0$). Using the modified polar coordinate system (ξ, θ) , where $\xi = \ln r$, the governing equations can be written in the form of the vorticity, stream function and energy equations as

$$e^{2\xi} \frac{\partial \zeta}{\partial t} = \frac{2}{Re} \left(\frac{\partial^2 \zeta}{\partial \xi^2} + \frac{\partial^2 \zeta}{\partial \theta^2} \right) - \frac{\partial \psi}{\partial \theta} \frac{\partial \zeta}{\partial \xi} + \frac{\partial \psi}{\partial \xi} \frac{\partial \zeta}{\partial \theta} \pm e^\xi \frac{Gr}{2Re^2} \left[\frac{\partial \phi}{\partial \xi} \sin \theta + \frac{\partial \phi}{\partial \theta} \cos \theta \right], \quad (1)$$

$$e^{2\xi} \zeta = \frac{\partial^2 \psi}{\partial \xi^2} + \frac{\partial^2 \psi}{\partial \theta^2}, \quad (2)$$

$$e^{2\xi} \frac{\partial \phi}{\partial t} = \frac{2}{Pe} \left(\frac{\partial^2 \phi}{\partial \xi^2} + \frac{\partial^2 \phi}{\partial \theta^2} \right) - \frac{\partial \psi}{\partial \theta} \frac{\partial \phi}{\partial \xi} + \frac{\partial \psi}{\partial \xi} \frac{\partial \phi}{\partial \theta}, \quad (3)$$

where t is the dimensionless time, ζ , ψ and ϕ are the dimensionless vorticity, stream functions and temperature, respectively, $Re = 2au_\infty/\nu$, is the Reynolds number, $Gr = g\beta(2a)^3(T_s - T_\infty)/\nu^2$ is the Grashof number, $Pe = Re Pr$, is the Péclet number, and Pr is the Prandtl number.

The dimensionless variables t, ζ, ψ and ϕ are defined as

$$t = t' u_\infty / a, \quad \zeta = -\zeta' a / u_\infty, \\ \psi = \psi' / a u_\infty, \quad \phi = (T - T_\infty) / (T_s - T_\infty),$$

where t', ζ', ψ' are the dimensional time, vorticity and stream function, respectively. The dimensionless radial and transverse velocity components v_r and v_θ are defined as

$$\left. \begin{aligned} v_r &= \frac{v'_r}{u_\infty} = \frac{1}{r} \frac{\partial \psi}{\partial \theta} = e^{-\xi} \frac{\partial \psi}{\partial \theta}, \\ v_\theta &= \frac{v'_\theta}{u_\infty} = -\frac{\partial \psi}{\partial r} = -e^{-\xi} \frac{\partial \psi}{\partial \xi}. \end{aligned} \right\} \quad (5)$$

It is important here to mention that the sign of the buoyancy term [the last term in equation (1)] depends on the flow regime and is positive for parallel flow and negative for contra flow.

The thermal boundary conditions are based on the constant temperature on the cylinder surface and the

free stream temperature away from it, and can be expressed as

$$\phi = 1 \quad \text{at} \quad \xi = 0 \quad \text{and} \quad \phi \rightarrow 0 \quad \text{as} \quad \xi \rightarrow \infty. \quad (6)$$

The boundary conditions of the velocity field are based on vanishing normal velocity as well as the no slip condition on the cylinder surface and the free stream conditions away from it. This will result in the following

$$\left. \begin{aligned} \psi = \frac{\partial \psi}{\partial \xi} = \frac{\partial \psi}{\partial \theta} = 0 \quad \text{at} \quad \xi = 0, \\ e^{-\xi} \frac{\partial \psi}{\partial \theta} \rightarrow \cos \theta, \quad e^{-\xi} \frac{\partial \psi}{\partial \xi} \rightarrow \sin \theta, \\ \xi \rightarrow 0 \quad \text{as} \quad \xi \rightarrow \infty. \end{aligned} \right\} \quad (7)$$

THE METHOD OF SOLUTION

The method used for solving the present problem is similar to that developed by Badr [6] to study the problem of cross mixed convection from a circular cylinder. In this method the velocity and thermal boundary layers are developed in time until reaching steady conditions. This has been achieved in two stages. During the first stage of motion the free stream is assumed to start from rest at $t = 0$ with no temperature difference between the cylinder surface and the approaching flow. In this stage the velocity boundary layer develops partially with time while no body forces present. The second stage starts at time $t = t^*$ at which the cylinder is assumed to be heated instantaneously to the constant surface temperature T_s . In this stage the velocity and thermal fields develop simultaneously with time until reaching steady conditions.

In case of parallel and contra mixed convection regimes the flow and temperature fields are symmetric about a vertical line passing through the cylinder centre. Accordingly the following series expansion of the stream function ψ , vorticity ζ and temperature ϕ is assumed

$$\psi = \sum_{n=1}^N f_n(\xi, t) \sin n\theta, \quad (8a)$$

$$\zeta = \sum_{n=1}^N g_n(\xi, t) \sin n\theta, \quad (8b)$$

$$\phi = \frac{1}{2} H_0(\xi, t) + \sum_{n=1}^N H_n(\xi, t) \cos n\theta. \quad (8c)$$

The same truncated Fourier series was used by Ingham [12] for studying the free convection limit ($Re = 0$) of the problem. Using equation (8) together with equation (2) will result in the following relation between the f_n and g_n functions

$$\frac{\partial^2 f_n}{\partial \xi^2} - n^2 f_n = e^{2\xi} g_n, \quad (9)$$

where $f_n = f_n(\xi, t)$ and $g_n = g_n(\xi, t)$. Similarly by using equations (8) with equations (1) and (3) the following differential equations can be deduced

$$2 e^{2\xi} \frac{\partial g_n}{\partial t} = \frac{4}{Re} \left(\frac{\partial^2 g_n}{\partial \xi^2} - n^2 g_n \right) \pm S_n, \quad (10a)$$

$$e^{2\xi} \frac{\partial H_0}{\partial t} = \frac{2}{Pe} \frac{\partial^2 H_0}{\partial \xi^2} + Z_0, \quad (10b)$$

$$2 e^{2\xi} \frac{\partial H_n}{\partial t} = \frac{4}{Pe} \left(\frac{\partial^2 H_n}{\partial \xi^2} - n^2 H_n \right) - n f_n \frac{\partial H_0}{\partial \xi} + Z_n, \quad (10c)$$

where S_n , Z_0 and Z_n are functions of ξ and t and defined as

$$\begin{aligned} S_n(\xi, t) = e^\xi \frac{Gr}{2Re^2} \left[-\delta_n \frac{\partial H_0}{\partial \xi} + \frac{\partial H_{n+1}}{\partial \xi} \right. \\ \left. - \frac{\partial H_{n-1}}{\partial \xi} + (n-1)H_{n-1} + (n+1)H_{n+1} \right] \\ + \sum_{m=1}^N \left\{ \frac{\partial g_m}{\partial \xi} (K f_K - J f_J) + m g_m \right. \\ \left. \times \left[\frac{\partial f_K}{\partial \xi} - \text{sgn}(m-n) \frac{\partial f_J}{\partial \xi} \right] \right\}, \end{aligned} \quad (11a)$$

$$Z_0(\xi, t) = - \sum_{n=1}^N n \left(f_n \frac{\partial H_n}{\partial \xi} + H_n \frac{\partial f_n}{\partial \xi} \right), \quad (11b)$$

$$\begin{aligned} Z_n(\xi, t) = - \sum_{m=1}^N \left\{ \frac{\partial H_m}{\partial \xi} (K f_K + J f_J) + m H_m \right. \\ \left. \times \left[\frac{\partial f_K}{\partial \xi} + \text{sgn}(m-n) \frac{\partial f_J}{\partial \xi} \right] \right\}, \end{aligned} \quad (11c)$$

where

$$\delta_n = \begin{cases} 1 & \text{when } n = 1 \\ 0 & \text{when } n \neq 1 \end{cases}, \quad K = m+n, \\ J = |m-n| \text{ and } \text{sgn}(m-n),$$

means the sign of the term $(m-n)$.

The boundary conditions of the functions f_n , g_n , H_0 and H_n are deduced from equations (6)–(8) and can be summarized as

$$\left. \begin{aligned} f_n = H_n = \frac{\partial f_n}{\partial \xi} = 0 \quad \text{and} \quad H_0 = 2 \quad \text{at} \quad \xi = 0, \\ g_n \rightarrow 0, \quad H_0 \rightarrow 0, \quad H_n \rightarrow 0 \quad \text{and} \\ f_n \rightarrow \delta_n e^\xi \quad \text{as} \quad \xi \rightarrow \infty. \end{aligned} \right\} \quad (12)$$

By integrating both sides of equation (9) with respect to ξ between $\xi = 0$ and ∞ and using the boundary conditions (12)

$$\int_0^\infty e^{(2-n)\xi} g_n d\xi = 2\delta_n. \quad (13)$$

The solution procedure and the details of the numerical technique used for solving equations (9) and (10) subjected to the boundary conditions (12) and satisfying the integral condition (13) are in principle similar to that used by Badr [6].

DISCUSSION OF RESULTS

Parallel flow

The problem of laminar combined convection from a hot horizontal circular cylinder is studied for the parallel flow regime at Reynolds numbers of 5, 20, 40

and 60 and at different values of Grashof number in each case. To be able to discuss and compare results the local and average Nusselt numbers, Nu and \overline{Nu} , are introduced such that

$$\left. \begin{aligned} Nu &= 2ah/k, \\ \overline{Nu} &= 2a\overline{h}/k, \end{aligned} \right\} \tag{14}$$

where h and \overline{h} represent the local and average heat transfer coefficients which were defined as

$$\begin{aligned} h &= \dot{q}/(T_s - T_\infty), \quad \overline{h} = \frac{1}{2\pi} \int_0^{2\pi} h \, d\theta, \\ \text{and } q &= -k \left(\frac{\partial T}{\partial r'} \right)_{r'=a}, \end{aligned} \tag{15}$$

where \dot{q} is the rate of heat transfer per unit area.

From equations (8), (14), and (15) it follows that

$$\left. \begin{aligned} Nu &= \left[-\frac{\partial H_0}{\partial \xi} - 2 \sum_{n=1}^{\infty} \frac{\partial h_n}{\partial \xi} \sin n\theta \right]_{\xi=0}, \\ \overline{Nu} &= - \left[\frac{\partial H_0}{\partial \xi} \right]_{\xi=0}. \end{aligned} \right\} \tag{16}$$

For all the cases considered, the calculated values of \overline{Nu} as well as the angle of separation θ_s are listed in Table 1. From Table 1 it can be seen that the value of Gr has no effect on the angle of separation for the case of $Re = 5$ since separation occurs at $\theta = 0$ and no circulation takes place in the wake. This criterion agrees with the results obtained by Collins and Dennis [13] who concluded the non-existence of re-circulating zones in the wake when $Re < 6$. At higher Reynolds numbers ($Re = 20, 40$ and 60) it was found that increasing Gr tends to delay flow separation. It can also be seen from Table 1 that, in the range of Re considered, the location of the point of separation depends on Re as well as Gr . In general, the same conclusion can be deduced from

Table 1. The average Nusselt number \overline{Nu} and the angle of separation θ_s for the case of parallel combined convection when $Pr = 0.7$

Re	Gr	\overline{Nu}	θ_s (deg.)
5	0	1.450	0.0
5	5	1.499	0.0
5	30	1.727	0.0
5	60	1.882	0.0
5	100	2.010	0.0
5	125	2.075	0.0
20	0	2.540	43.13
20	100	2.654	29.51
20	400	2.970	0.0
20	800	3.227	0.0
20	1200	3.420	0.0
20	1600	3.564	0.0
40	0	3.480	53.60
40	400	3.650	42.46
40	1600	4.100	0.0
40	3200	4.420	0.0
40	4800	4.690	0.0
40	6400	4.910	0.0
60	900	4.260	50.01
60	3600	4.912	23.29
60	7200	5.270	0.0

equation (1) since $Re, Gr/Re^2$ and the flow direction are the three parameters affecting the vorticity field.

The vorticity distribution around the cylinder surface at $Re = 20$ and 40 and for different values of Gr can be seen in Figs. 1(a) and (b). It is clear from Figs. 1(a) and (b) that increasing Gr tends to a significant increase in the surface vorticity. For example, the maximum surface vorticity for the cases of $Re = 20$ and 40 increased to three times its value by increasing the term Gr/Re^2 from 0 to 4. The locations of the point of separation when $Gr = 0$ (no heat transfer) for the two cases of $Re = 20$ and 40 are compared with the results of Dennis and Chang [14] and an excellent agreement is found. The angles of separation θ_s are not compared with those obtained by Merkin [5] since Merkin's results are based on the solution of the boundary-layer equations with the assumption of potential flow

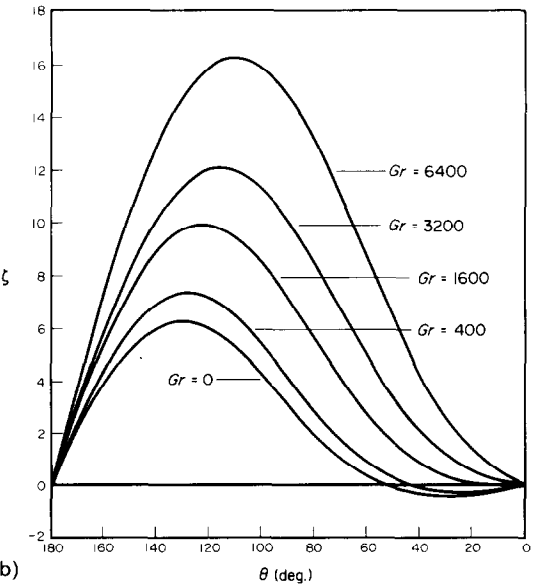
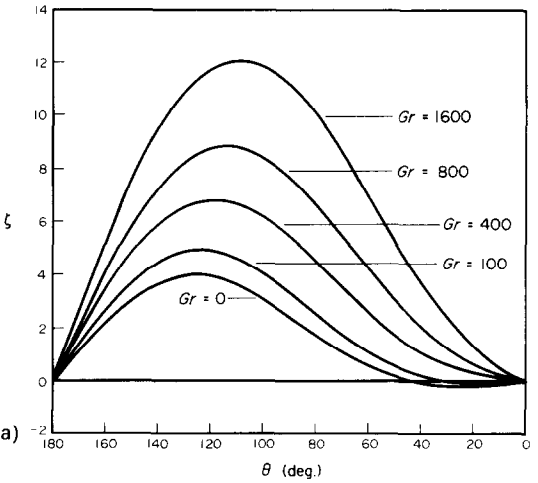


FIG. 1. The vorticity distribution on the cylinder surface at different values of Gr for the case of parallel flow when $Pr = 0.7$ and (a) $Re = 20$, (b) $Re = 40$.

prevailing outside the boundary layer. It is important here to mention that, in the considered range of Reynolds numbers ($Re \leq 60$), the full equations of motion are utilized and not the boundary-layer equations due to the following reasons. First, the boundary-layer thickness is not small especially at low Re or when the forced flow direction is opposite to that of natural convection. Second, the boundary-layer approximation is no longer valid in all cases in the region following the point of separation (wake region). Third, there is no way to predict, accurately enough, the velocity distribution outside the boundary layer especially for the case of contra flow when the term $Gr/Re^2 \sim O(1)$.

In the two studies (refs. [2, 5]), the boundary-layer approximations were considered for parallel and contra flow regimes. In both studies the potential flow is assumed outside the boundary layer. As a result of these approximations and assumptions it was found that the angle of separation depends only on the ratio Gr/Re^2 and not on Re . It is believed that this criterion might be true for parallel flow at high Reynolds number but not in the range of Re considered in this work.

Table 1 also shows that \bar{Nu} , at a given Re , increases continuously with the increase of Gr for parallel flows. This is a natural result of the increase of the vorticity all over the cylinder surface as demonstrated in Fig. 1. The local Nusselt number distributions for the two cases of $Re = 20$ and 40 and at different values of Gr in each case are shown in Figs. 2(a) and (b). It can be seen from Figs. 2(a) and (b) that increasing Gr results in a significant increase in Nu near the front stagnation point ($\theta = 180^\circ$). The response of the local Nusselt number to the increase in Gr near the rear stagnation point is slightly different. At first, a small increase in Gr above its zero value causes a decrease in the local Nusselt number until reaching its minimum value. A further increase in Gr results in increasing Nu near $\theta = 0^\circ$. The reason for this behaviour is that the initial increase of Gr above its zero causes a decrease in $|\zeta|$ near $\theta = 0^\circ$ [see Figs. 1(a) and (b)] and accordingly causes a drop in Nu . Further increase in Gr results in increasing $|\zeta|$ near $\theta = 0^\circ$ and accordingly increasing Nu there.

In Figs. 2(a) and (b) the forced convection Nusselt number distribution is compared with that obtained by Dennis *et al.* [15] at the same value of Re but at $Pr = 0.73$ instead of $Pr = 0.7$ considered in the present study. Figure 3 shows a comparison between the predicted values of \bar{Nu} and the experimental correlation of Hatton *et al.* [7]. In Hatton's correlation \bar{Nu} is expressed as a function of an effective Reynolds number Re_{eff} that is defined for the case of parallel flow as

$$Re_{eff} = Re [1 + (2.06 Ra^{0.418}/Re) + (1.06 Ra^{0.836}/Re^2)],$$

where Ra is the Rayleigh number ($= Gr Pr$). The difference in \bar{Nu} between Hatton's correlation and the present results did not exceed 11%. This difference is believed to be due to the uncertainty in the experimental measurements, the limitation of Hatton's

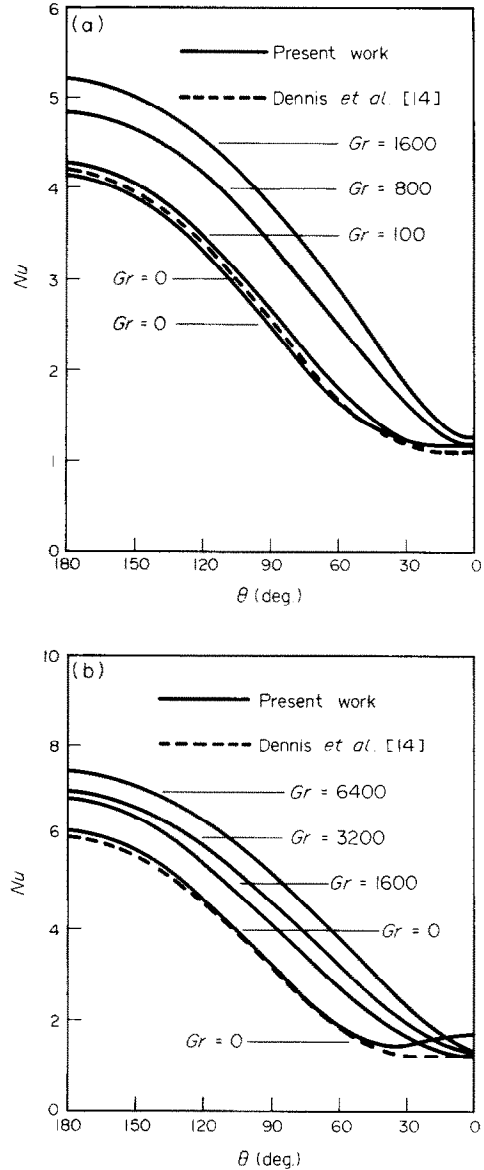


FIG. 2. Variation of the local Nusselt number on the cylinder surface for the case of parallel flow when $Pr = 0.7$ and a comparison with the results obtained by Dennis *et al.* [14] for the special case of forced convection for (a) $Re = 20$, and (b) $Re = 40$.

correlation to a range of Gr that is far below most of those considered in this work and the assumption of constant fluid properties. The results are also plotted on the same coordinates used in refs. [9, 10] as can be seen in Fig. 4. If the present theoretical results are to be fitted to a single curve the following equation, which is of the form suggested by Jackson and Yen [10], can be used

$$\frac{\bar{Nu}}{\bar{Nu}_{forced}} = \left[1 + \frac{Gr}{Re^2} \right]^{0.2133} \quad (17)$$

The streamline and isotherm patterns for the cases of $Re = 20$ and 40 and for different values of Gr can be seen in Figs. 5(a) and (b) and 6(a) and (b). It is found from the

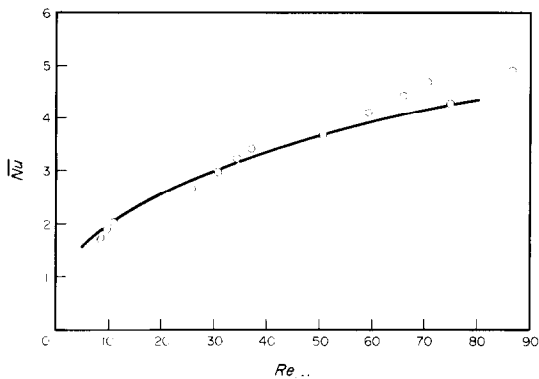


FIG. 3. Comparison between the present results, O; and the experimental correlation obtained by Hatton *et al.* [7], — for the case of parallel flow.

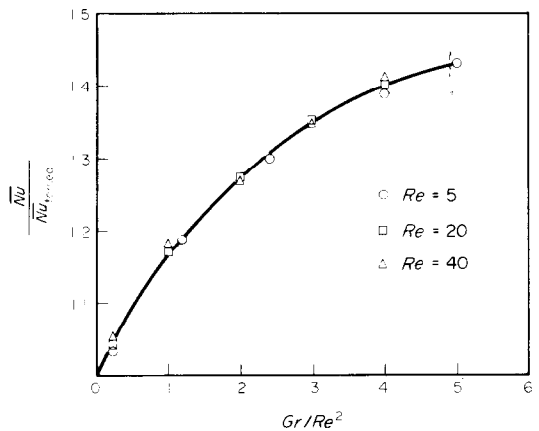


FIG. 4. The effect of the parameter Gr/Re^2 on the ratio between the Nusselt numbers of combined and forced convection regimes for the case of parallel flow.

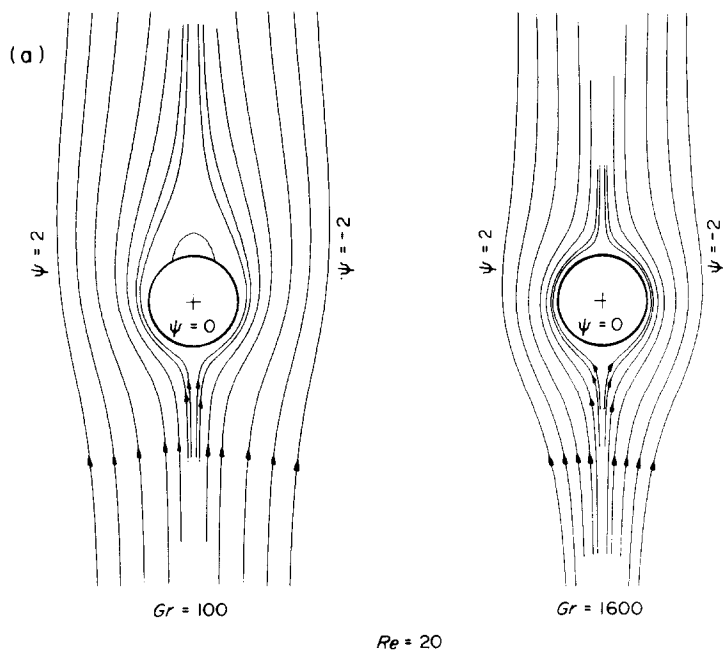
Table 2. The average Nusselt number \overline{Nu} and the angle of separation θ_s for the case of contra combined convection when $Pr = 0.7$

Re	Gr	\overline{Nu}	θ_s (deg.)
5	5	2.37	31.33
5	10	1.19	67.74
5	25	1.12	180.00
20	100	2.12	62.84
20	400	1.78	144.82
20	800	2.15	180.00
40	400	3.17	68.33
40	800	3.05	79.19
40	1600	2.70	106.77
40	3200	3.22	180.00

streamline plots for the parallel flow regime that increasing Gr results in decreasing the wake length until it completely disappears. The isotherm patterns for the same cases [see Figs. 6(a) and (b)] show that as Gr increases the $\phi = 0.9$ line gets closer to the cylinder surface which indicates higher temperature gradient and accordingly higher heat transfer rates. Figures 5(a) and (b) and 6(a) and (b) show also the dependence of the velocity and temperature fields not only on the ratio Gr/Re^2 but also on the value of Re .

Contra flow

The contra flow combined convection regime is studied at Reynolds numbers of 5, 20 and 40 and at different values of Gr in each case. Table 2 shows the predicted values of \overline{Nu} as well as θ_s for each of the various cases considered. It is clear from the results that increasing Gr above its zero value causes the average Nusselt number to decrease significantly due to the slow down of the flow velocity near the cylinder surface.



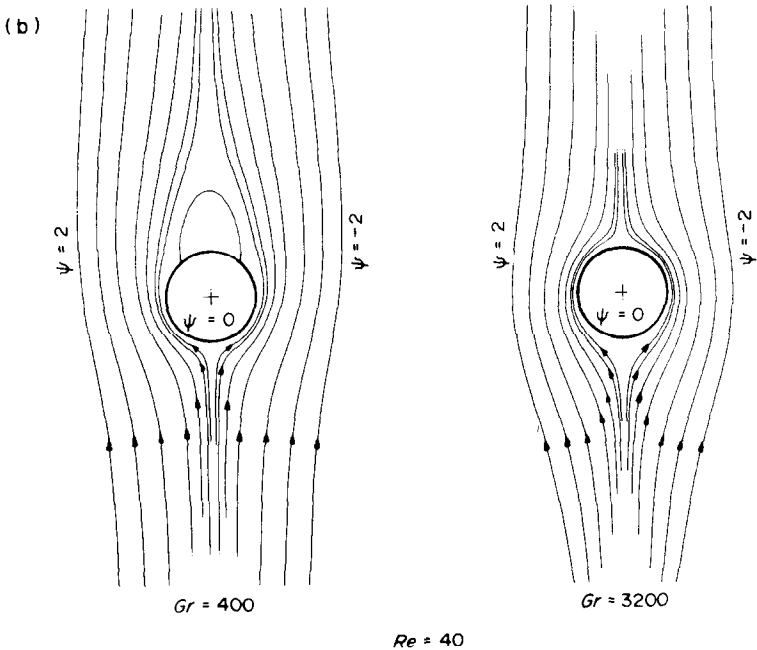


FIG. 5. Streamline patterns for the parallel flow regime when $Pr = 0.7$ and (a) $Re = 20$, (b) $Re = 40$. (The shown streamlines are $\psi = -2.0, -1.5, -1.0, -0.5, -0.25, -0.1, -0.05, 0, 0.05, 0.1, 0.25, 0.5, 1.0, 1.5$, and 2.0 .)

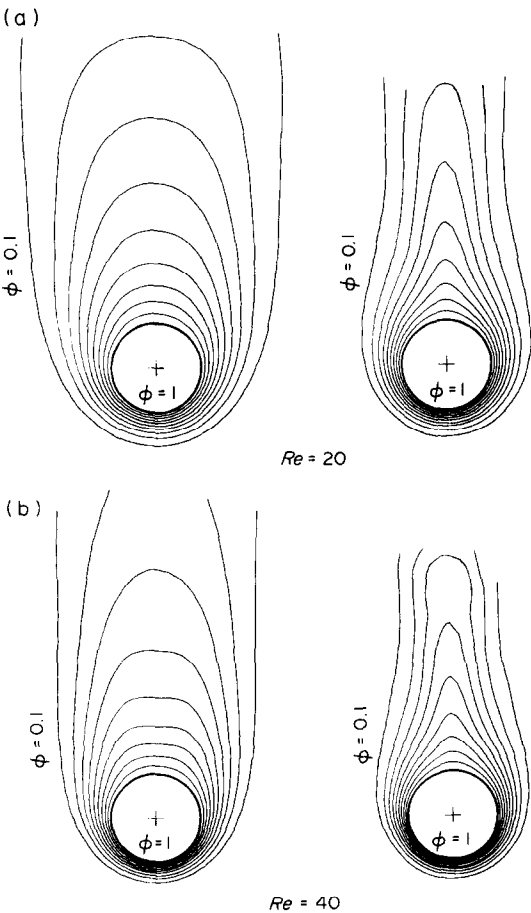


FIG. 6. Isotherms for the parallel flow regime when $Pr = 0.7$ and (a) $Re = 20$, (b) $Re = 40$. (The shown isotherms are $\phi = 1, 0.9, 0.8, \dots$, and 0.1 .)

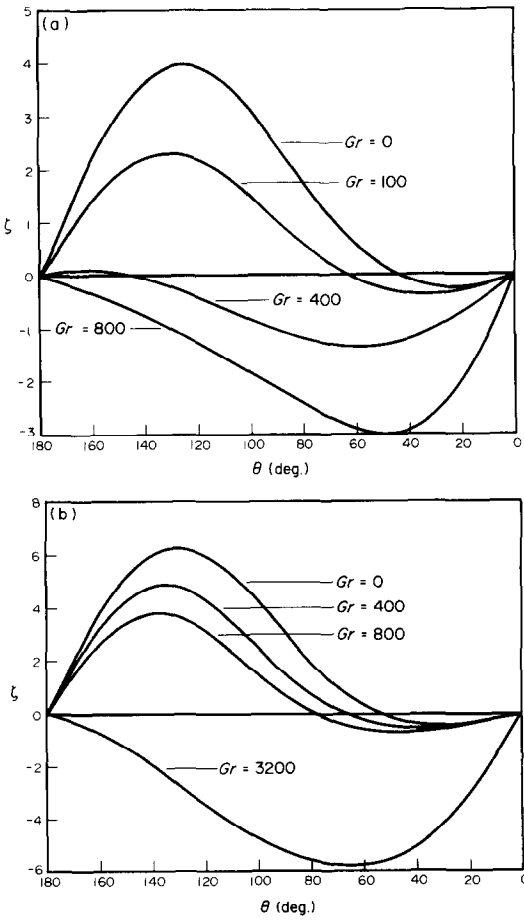


FIG. 7. The vorticity distribution on the cylinder surface at different values of Gr for the contra flow regime when $Pr = 0.7$ and (a) $Re = 20$, (b) $Re = 40$.

Further increase in Gr results in an increase of \overline{Nu} and the flow field becomes more dominated by natural convection.

The effect of Gr on the vorticity distribution around the cylinder surface can be seen in Figs. 7(a) and (b). Although ζ decreases over all the surface as Gr increases, the value of $|\zeta|$ increases near $\theta = 0^\circ$ (the backward stagnation point). This is mainly because the buoyant forces are aiding the circulating flow close to the cylinder surface near $\theta = 0^\circ$. This effect causes Nu to increase with the increase of Gr in the same region while decreasing in the region surrounding the forward stagnation point ($\theta = 180^\circ$) as can be seen in Figs. 8(a) and (b). It can also be seen from Figs. 7(a) and (b) as well as Table 2 that increasing Gr causes the point of separation ($\zeta = 0$) to move towards the forward stagnation point contrary to the case of parallel flow.

The streamlines and isotherms for the contra flow regime at $Re = 20$ and 40 and at different values of Gr are shown in Figs. 9(a) and (b) and 10(a) and (b). As expected, the geometry of the wake region is completely different from that occurring in the parallel flow regime at the same values of Re and Gr/Re^2 . At low values of Gr the wake takes place at the downstream side of the cylinder. The circulating fluid in the wake is completely isolated from the main flow and heat is transferred from this region to the main stream by conduction across the wake boundaries. As Gr increases the wake gets bigger [see Figs. 9(a) and (b)] until the wake boundaries completely surround the cylinder forming a cylindrical dome. The circulating fluid inside the dome is driven by the buoyant forces and never gets entrained to the main stream. In this case, the heat transfer from the cylinder surface becomes influenced by natural convection inside the dome. Similar to the wake region, heat is transferred from the circulating fluid inside the dome to the main stream by conduction through the dome boundaries.

CONCLUSION

The problem of laminar combined convection heat transfer from a hot horizontal circular cylinder is studied for the two cases of parallel and contra flow regimes. The full governing equations of motion and energy are solved in order to predict the details of the velocity and thermal boundary layers. The variations of vorticity and local Nusselt number are obtained over all the cylinder surface including the zone beyond the

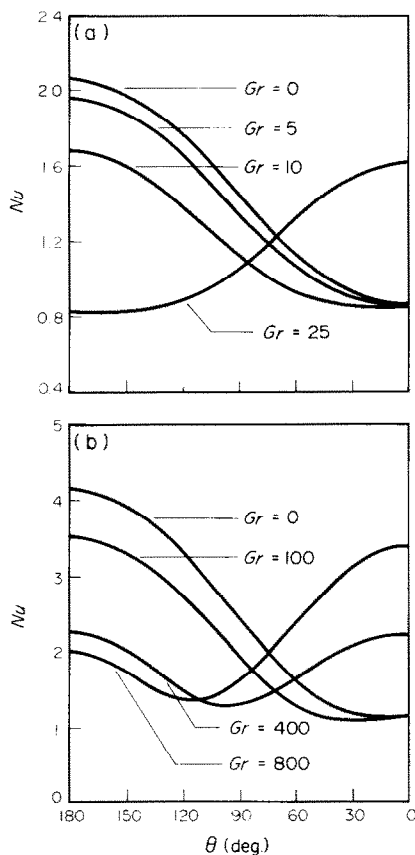


FIG. 8. Variation of the local Nusselt number on the cylinder surface for the case of contra flow when $Pr = 0.7$ and (a) $Re = 5$, (b) $Re = 20$.

point of separation. The effect of increasing Grashof number on the vorticity and Nusselt number distributions for both cases of parallel and contra flows are discussed in detail. The predicted values of the average Nusselt number are compared with the available experimental correlations and a satisfactory agreement is found. The streamlines and isotherms are plotted for different Reynolds and Grashof numbers to show some of the details of the velocity and thermal fields.

Acknowledgement—The author wishes to acknowledge the support received from the University of Petroleum & Minerals during this study.

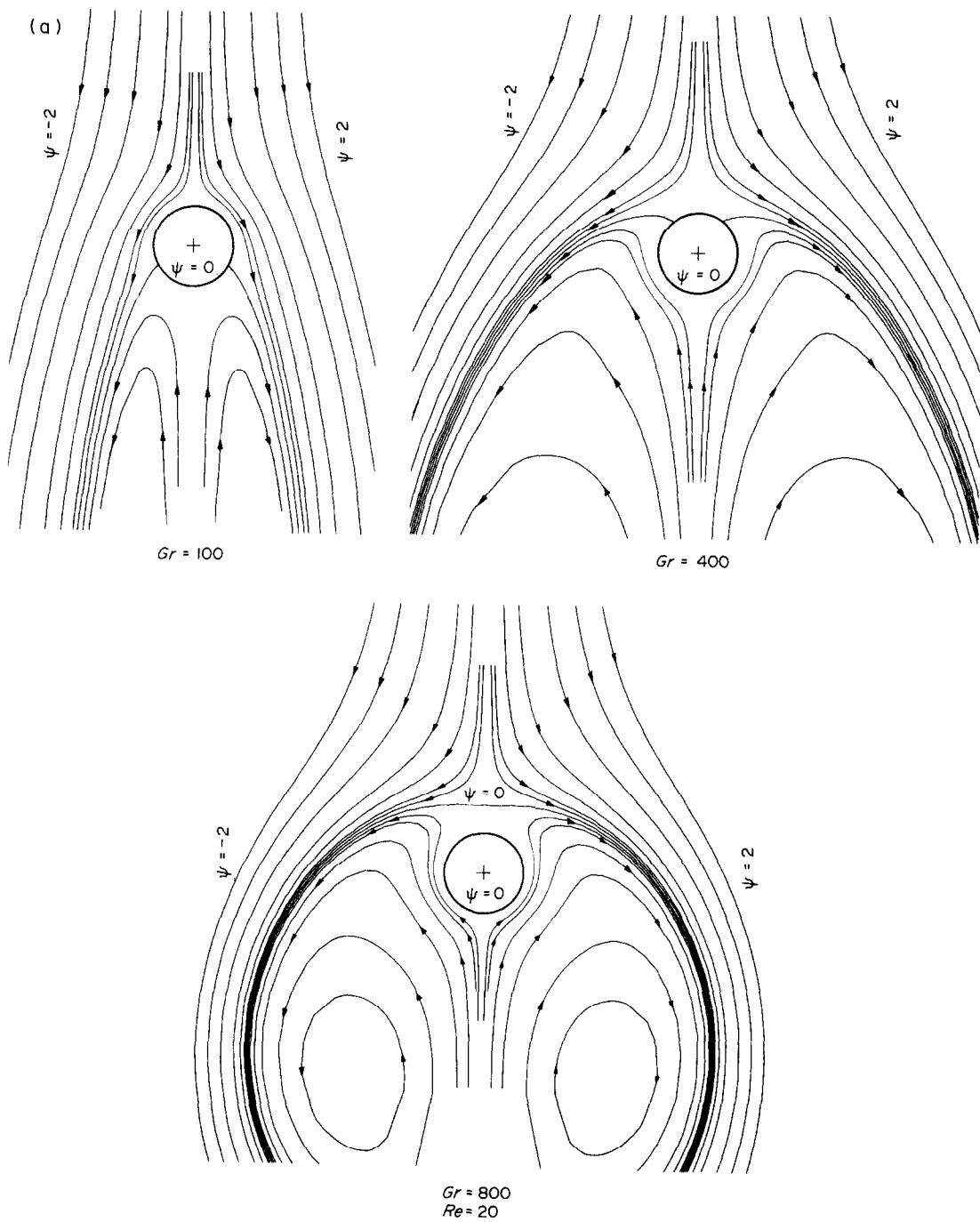


FIG. 9(a).

[continued overleaf]

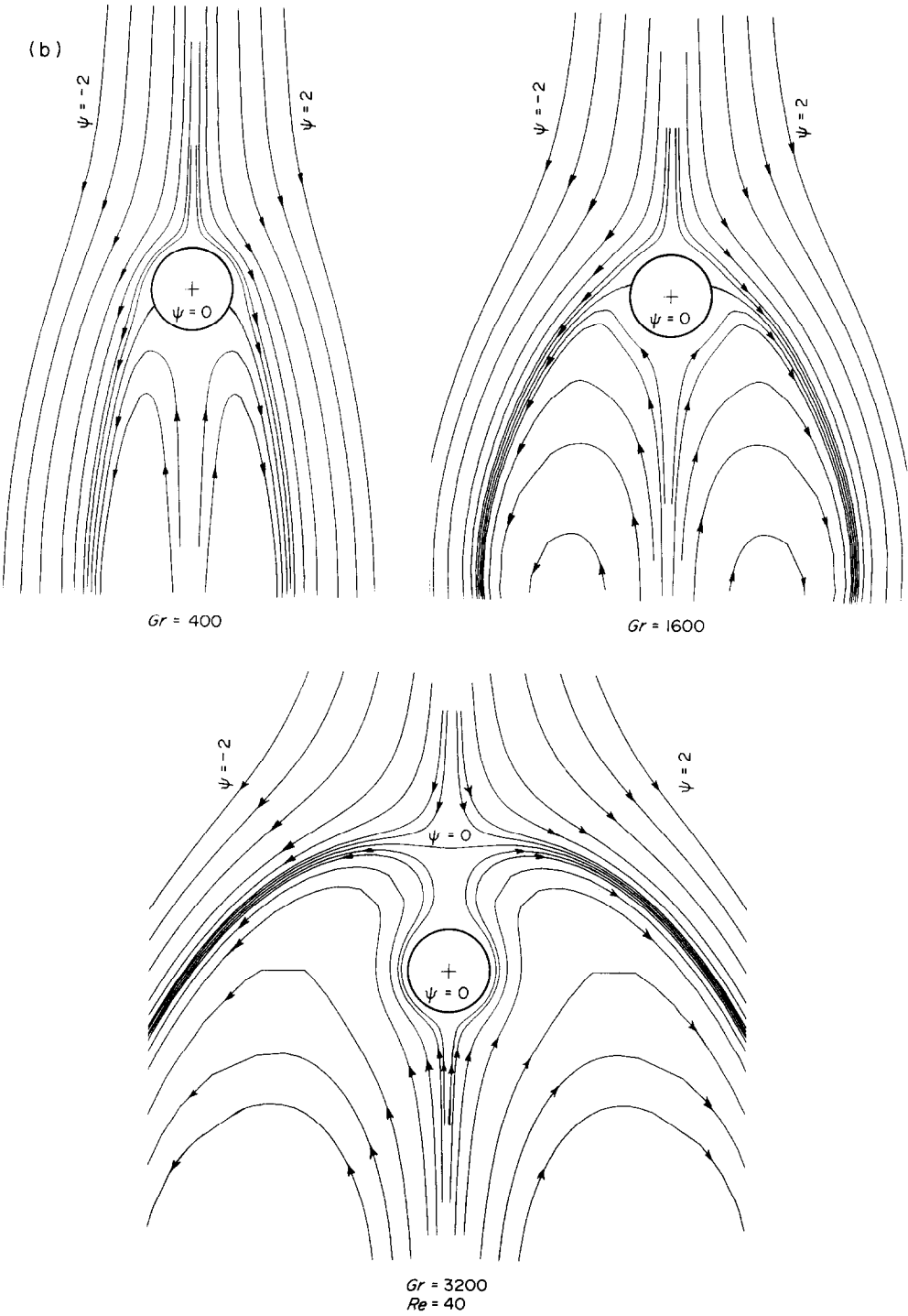


FIG. 9. Streamline patterns for the contra flow regime when $Pr = 0.7$ and (a) $Re = 20$, (b) $Re = 40$. (The shown streamlines are $\psi = -2.0, -1.5, -1.0, -0.5, -0.25, -0.1, -0.05, 0, 0.05, 0.1, 0.25, 0.5, 1.0, 1.5, 2.0$.)

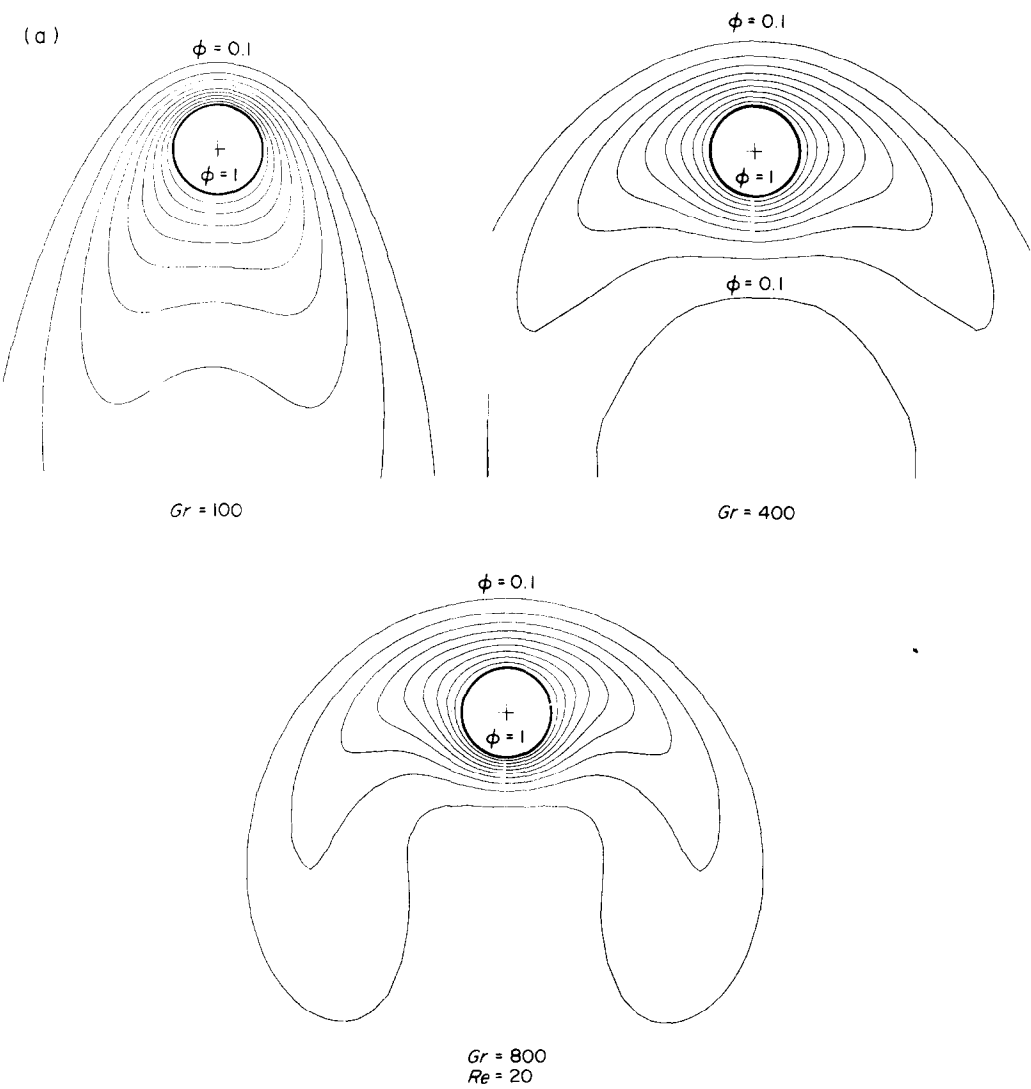


FIG. 10(a).

[continued overleaf]

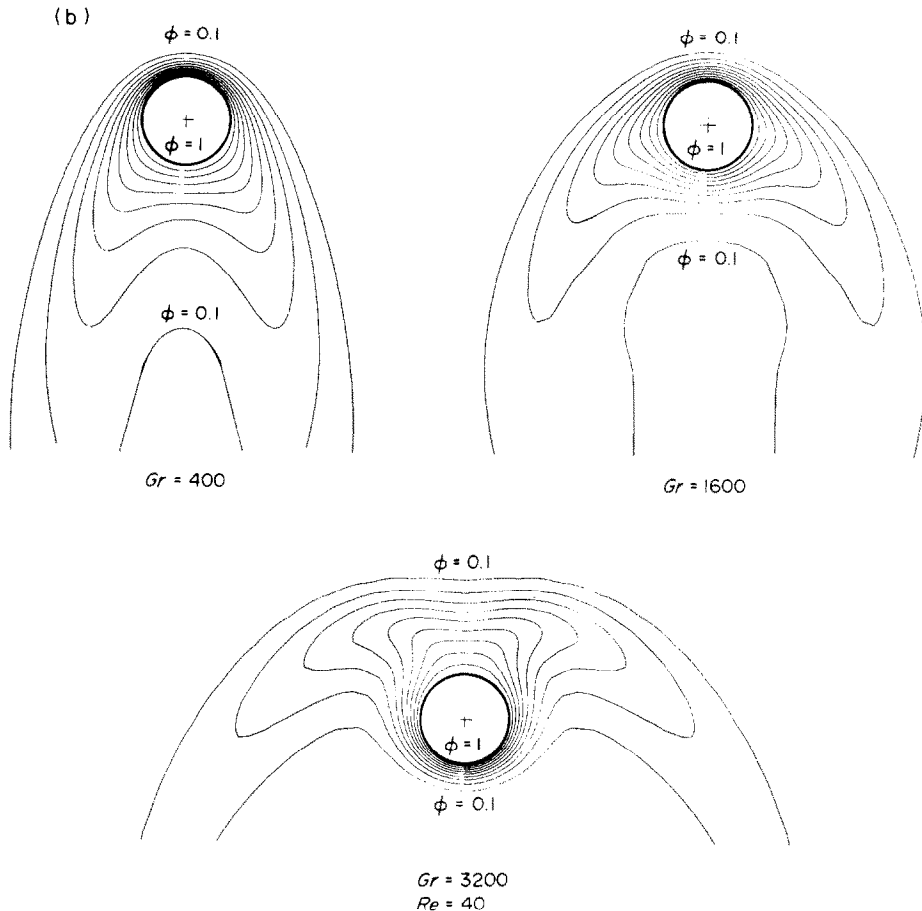


FIG. 10. Isotherms for the contra flow regime when $Pr = 0.7$ and (a) $Re = 20$, (b) $Re = 40$. (The plotted isotherms are $\phi = 1, 0.9, 0.8, \dots$, and 0.1 .)

REFERENCES

1. A. Acrivos, On the combined effect of forced and free convection heat transfer in laminar boundary layer flows, *Chem. Engng Sci.* **21**, 343–352 (1966).
2. N. D. Joshi and S. P. Sukhatme, An analysis of combined free and forced convection heat transfer from a horizontal circular cylinder to a transverse flow, *J. Heat Transfer* **93**, 441–448 (1971).
3. S. Nakai and T. Okazaki, Heat transfer from a horizontal circular wire at small Reynolds and Grashof numbers—II, *Int. J. Heat Mass Transfer* **18**, 397–413 (1975).
4. E. M. Sparrow and L. Lee, Analysis of mixed convection about a horizontal cylinder, *Int. J. Heat Mass Transfer* **19**, 229–232 (1976).
5. J. H. Merkin, Mixed convection from a horizontal circular cylinder, *Int. J. Heat Mass Transfer* **20**, 73–77 (1976).
6. H. M. Badr, A theoretical study of laminar mixed convection from a horizontal cylinder in a cross stream, *Int. J. Heat Mass Transfer* **26**, 639–653 (1983).
7. A. P. Hatton, D. D. James and H. W. Swire, Combined forced and natural convection with low-speed air flow over horizontal cylinders, *J. Fluid Mech.* **42**, 17–31 (1970).
8. B. Gebhart and L. Pera, Mixed convection for long horizontal cylinders, *J. Fluid Mech.* **45**, 49–64 (1970).
9. P. H. Oosthuizen and S. Madan, Combined convection heat transfer from horizontal cylinders in air, *J. Heat Transfer* **92**, 194–196 (1970).
10. T. W. Jackson and H. H. Yen, Combined forced and free convective equations to represent combined heat-transfer coefficients for horizontal cylinders, *J. Heat Transfer* **93**, 247–248 (1971).
11. P. H. Oosthuizen and S. Madan, The effect of flow direction on combined convective heat transfer from cylinders to air, *J. Heat Transfer* **93**, 240–242 (1971).
12. D. B. Ingham, Free convection boundary layer on an isothermal horizontal cylinder, *Z. Angew. Math. Phys.* **29**, 871–883 (1978).
13. W. M. Collins and S. C. R. Dennis, Flow past an impulsively started circular cylinder, *J. Fluid Mech.* **60**, 105–127 (1973).
14. S. C. R. Dennis and G. Chang, Numerical solutions for steady flow past a circular cylinder at Reynolds numbers up to 100, *J. Fluid Mech.* **42**, 471–489 (1970).
15. S. C. R. Dennis, J. D. Hudson and N. Smith, Steady laminar forced convection from a circular cylinder at low Reynolds numbers, *Physics Fluids* **11**, 933–940 (1967).

CONVECTION LAMINAIRE MIXTE AUTOUR D'UN CYLINDRE HORIZONTAL AVEC DES REGIMES D'ÉCOULEMENT FAVORABLE OU ADVERSE

Résumé—La convection laminaire mixte de la chaleur à partir d'un cylindre circulaire horizontal est étudiée pour les deux cas de l'écoulement forcé dirigé soit vers le haut (écoulement favorable) soit vers le bas (écoulement adverse). L'étude est basée sur la résolution de l'équation de transport de vorticit ,   partir de la fonction de courant, et de l' quation de l' nergie. Les couches limites dynamique et thermique sont d velopp es dans le temps jusqu'  l'obtention des conditions permanentes. Les variations de la vorticit  et du nombre de Nusselt sont obtenues sur toute la surface du cylindre en incluant la zone voisine du point de s paration. Les valeurs th oriques du nombre de Nusselt moyen sont compar es aux donn es exp rimentales disponibles et l'accord est satisfaisant. Les configurations des lignes de courant et des isothermes sont trac es pour quelques cas afin de montrer quelques caract ristiques du champ d' coulement.

LAMINARE  BERLAGERTE KONVEKTION AN EINEM WAAGERECHTEN ZYLINDER IM GLEICH- UND GEGENSTROM

Zusammenfassung—Der W rme bergang bei laminarer  berlagerter freier und erzwungener Konvektion an einem isothermen waagerechten Zylinder wird f r die beiden F lle der aufw rtsgerichteten (Gleichstrom) und abw rtsgerichteten Konvektionsstr mung (Gegenstrom) untersucht. Die Untersuchung basiert auf der L sung der vollst ndigen Wirbeltransportgleichung zusammen mit der L sung der Stromfunktion und der Energiegleichung. Die Geschwindigkeits- und Temperaturgrenzschichten werden zeitabh ngig entwickelt, bis station rer Zustand erreicht ist. Die  nderungen der Wirbelintensit t und der Nusselt-Zahl werden  ber die gesamte Zylinderoberfl che einschlie lich des Gebiets nach dem Abl sungspunkt ermittelt. Die berechneten Werte der mittleren Nusselt-Zahl werden mit vorhandenen Versuchsergebnissen verglichen. Die  bereinstimmung ist zufriedenstellend. Stromlinien- und Isothermenfelder werden dargestellt, um einige typische Eigenschaften der Str mungsfelder zu zeigen.

ЛАМИНАРНАЯ СМЕШАННАЯ КОНВЕКЦИЯ ОТ ГОРИЗОНТАЛЬНОГО ЦИЛИНДРА—РЕЖИМЫ СПУТНОГО И ПРОТИВОТОЧНОГО ТЕЧЕНИЙ

Аннотация—Теплоперенос при ламинарной смешанной конвекции от изотермического горизонтального кольцевого цилиндра исследуется в двух случаях: (а) поток вынужденной конвекции направлен вертикально вверх (спутный поток) и (б) – вертикально вниз (противоток). Исследование основано на решении полного уравнения переноса завихренности вместе с уравнениями для функции тока и энергии. Динамические и тепловые пограничные слои развиваются во времени до достижения стационарного состояния. Определены изменения завихренности и числа Нуссельта по всей поверхности цилиндра, включая зону за точкой отрыва потока. Проведено сравнение расчетных значений среднего числа Нуссельта с имеющимися экспериментальными данными и получено их удовлетворительное совпадение. Дано графическое представление линий тока и изотерм для ряда случаев с целью иллюстрации некоторых характеристик поля течения.